Agricultural and Forest Meteorology 150 (2010) 1597–1606

Contents lists available at ScienceDirect

Agricultural and Forest Meteorology

journal homepage: www.elsevier.com/locate/agrformet

Testing the performance of a novel spectral reflectance sensor, built with light emitting diodes (LEDs), to monitor ecosystem metabolism, structure and function

Youngryel Ryu[a,*,1], Dennis D. Baldocchi[a], Joseph Verfaillie[a], Siyan Ma[a], Matthias Falk[b], Ilse Ruiz-Mercado[c], Ted Hehn[d], Oliver Sonnentag[a,1]

[a] Department of Environmental Science, Policy and Management, University of California, Berkeley, CA, USA
[b] Department of Land, Air and Water Resources, University of California, Davis, CA, USA
[c] Department of Civil and Environmental Engineering, University of California, Berkeley, CA, USA
[d] NEON Inc., Boulder, CO, USA

ARTICLE INFO

Article history:
Received 31 March 2010
Received in revised form 18 August 2010
Accepted 19 August 2010

Key words:
Light emitting diode
Spectral reflectance
Phenology
Canopy photosynthesis
Leaf area index
NDVI

ABSTRACT

We developed and tested the use of light emitting diodes (LEDs) to monitor vegetation reflectance in narrow spectral bands as a tool suitable for quantifying and monitoring ecosystem structure, function and metabolism. LEDs are appealing because they are inexpensive, small and reliable light sources that, when used in reverse mode, can measure spectrally selective radiation. We selected LEDs in red and near-infrared wavebands as they are used to calculate the normalized difference vegetation index (NDVI). The lab experiments revealed that the LEDs showed linear relation with a hyper-spectral spectroradiometer ($R^2 > 0.94$ and 0.99 for red and NIR, respectively) and marginal sensitivity to temperature. To test the efficacy of this novel sensor, we measured spectral reflectance with LEDs over an annual grassland in California over 3.5 years. The LED-sensor captured daily to interannual variation of the spectral reflectance at the two bands with reliable and stable performance. The spectral reflectance in the two bands and NDVI proved to be useful to identify the leaf-on and leaf-off dates (mean bias errors of 5.3 and 4.2 days, respectively) and to estimate canopy photosynthesis ($R^2 = 0.91$). We suggest that this novel instrument can monitor other structural and functional (e.g. leaf area index, leaf nitrogen) variables by employing LEDs that have other specific wavelengths bands. Considering that off-the-shelf LEDs cover a wide range of wavebands from the ultraviolet to near-infrared regions, we believe that the research community could explore a range of similar instruments across a range of bands for a variety of ecological applications.

1. Introduction

Linking spectral reflectance indices with vegetation structure (e.g. leaf area index (LAI)), function (e.g. nitrogen (N), phenology) and metabolism (e.g. gross primary productivity, evaporation) has advanced the understanding of ecosystem processes and their influence on biosphere-atmosphere interactions (Baldocchi et al., 1996; Gamon et al., 2006b; Running et al., 1999). The reflectance of solar radiation in the visible and near-infrared portions of the electromagnetic spectrum is correlated with vegetation status, development and growth, and is monitored for this reason in remote sensing of terrestrial vegetation. Spectral reflectance measured from air- and space-borne platforms covers broad areas repeatedly, but such measurements are prone to contamination by atmospheric effects (e.g. aerosol, clouds, etc.) (Kobayashi and Dye, 2005). Thus, continuous observation of vegetation reflectance *in situ* is warranted to better understand the vegetation status with direct high spatial and temporal resolution data (Gamon et al., 2006b).

Efforts to monitor vegetation spectral reflectance continuously have been initiated in several studies, including sophisticated multi-angle hyper-spectrometer (Hilker et al., 2007; Leuning et al., 2006), a rotating hemispherical spectrometer (Nagai et al., 2010) and a dual detector spectrometer attached to a mobile tram system (Gamon et al., 2006a). However, commercially available spectrometers used in the previous studies are expensive. The combination of PAR and solar radiation sensors was used as a proxy of NDVI, but their broad wavebands caused narrow range of NDVI comparing to the narrowband NDVI sensor (Huemmrich et al., 1999). Recently, a narrow-band spectrometer equipped with photodiodes in a moderate cost ($720 per pair) was reported (Garrity et al., 2010). That system requires narrow-bandpass filters to measures spectral reflectance for specific wavebands and the cost of the fil-

* Corresponding author at: 130 Mulford Hall #3114, University of California, Berkeley, CA 94720-3114, USA. Tel.: +1 510 642 9048; fax: +1 510 643 5098.
E-mail addresses: ryuyr77@gmail.com, yryu@berkeley.edu (Y. Ryu).
[1] Present address: Department of Organismic and Evolutionary Biology, Harvard University, HUH 22 Divinity Ave, Cambridge, MA 02138, USA.

0168-1923/$ – see front matter © 2010 Elsevier B.V. All rights reserved.
doi:10.1016/j.agrformet.2010.08.009

ters constitute a large portion of the total price (Garrity et al., 2010). Alternatively, light emitting diodes (LEDs) have the potential to measure vegetation spectral reflectance for a wide range of narrow and selective wavebands without the use of narrow-bandpass filters (RayChaudhuri and Sen, 2009). In particular, their low price (several dollars per LED) has much appeal.

Light emitting diodes are semiconductor devices that generate incoherent light in narrow spectral bands when an external voltage applied across the semiconductor junction allows a sufficient amount of high energy electrons to recombine with holes, producing light by spontaneous emission (Acharya et al., 1995). Conversely, when light in a given energy bandwidth is applied into the junction, electron-hole pairs are generated and a photocurrent produced. Atmospheric scientists applied this principle to monitor precipitable water over 10 years with very reliable stability (Brooks and Mims, 2001; Mims, 1992, 2002). However, the application of LEDs to monitor vegetation reflectance is at the very beginning.

LEDs have the potential to provide multi-band reflectance because commercially available LEDs exist for many wavelength bands, including ultraviolet, blue, green, red, and near-infrared. Valuable information can be inferred from multispectral reflectance in ecological studies because numerous aspects of ecosystem structure, function and metabolism show wavelength-specific responses (Asner and Martin, 2009; Sellers, 1985; Ustin et al., 2004). Thus it is possible to construct a spectrometer that combines LEDs covering different wavelength bands to monitor specific ecological processes.

There has been pressing need to monitor phenology (Morisette et al., 2009) because length of growing season modulates annual carbon uptake (Baldocchi et al., 2001; Black et al., 2000; Carrara et al., 2003) and evaporation (Ryu et al., 2008) of ecosystems and because phenology produces an independent signature of climate change (Parmesan and Yohe, 2003; Peñuelas et al., 2009). Inferring phenological events based on satellite-derived spectral reflectance has been widely used with moderate spatial (several km) and temporal (8-day or half-monthly) resolutions (White et al., 2009). *In situ* optical sensors have been used to quantify canopy structure (Leblanc et al., 2005; Ryu et al., 2010a,b) but the regular use for monitoring phenology has been limited due to logistic constraints (Barr et al., 2004). LEDs have the potential to continuously monitor phenology with high spatial and temporal resolutions at the field scale.

In this study, we examine the performance of a novel LED-sensor that we designed, built and tested for 3.5 years over an annual grassland of California. In this paper, we describe the novel LED-sensor and test its performance in the lab and in the field and investigate how the instrument allows us to answer a variety of remote sensing science questions on its utility to predict variables related to vegetation structure, function and metabolism using a multi-year data set. Specifically, we address three scientific questions including: (1) How does solar zenith angle influence spectral reflectance and NDVI of the LED-sensor? (2) Can this new instrument monitor seasonal and interannual variations of vegetation spectral reflectance? (3) Can the new instrument track temporal changes in ecosystem phenology? and (4) Can the instrument be used to estimate the canopy photosynthesis, LAI and N for an annual grassland?

2. Developing and testing of LED-sensor

2.1. Study site

The study site is an annual grassland (Vaira Ranch, latitude: 38.413°N; longitude: 120.951°W; altitude: 129 m) in central California, USA (Ryu et al., 2008). It experiences a Mediterranean-type climate with dry hot summers and wet mild winters. Precipitation is concentrated between November and May with little precipitation during the summer. The grass is dominated by cool-season C_3 annual species, including *Brachypodium distachyon* L., and *Hypochaeris glabra* L. (Ma et al., 2007; Xu and Baldocchi, 2004). Grasses usually germinate around November with the beginning of winter rainfall and grow between December and May, followed by quick senescence with the onset of the summer drought.

2.2. Development of LED-sensor

2.2.1. Description of LED-sensor

We developed the LED-sensor in 2004. In general, LEDs are used as photo detectors and produce a relatively high voltage (~1VDC) that is non-linear with intensity. In reverse mode they produce a small current (micro-amps) that is linear with intensity of incident light (RayChaudhuri and Sen, 2009). To measure this current, a chopper-stabilized and low temperature coefficient operational amplifier (op-amp LTC1050) was used as an inverting amplifier where $V_{out} = -I_{in} \times R_f$. That is, the voltage out (V_{out}) equals the negative current in (from the LED, $-I_{in}$) times the feedback resistor (R_f). Two LEDs were wired in parallel to double the base current and connected in reverse polarity to the op-amp to correct the sign of the output voltage. The op-amps required power and this was supplied with a DC/DC power supply that accepts a wide range of input voltages (9–36VDC) and outputs very stable 12VDC power. The voltage outputs from the op-amps were read by a Campbell data logger (CR23x) once every 10 s and recorded as 30 min averages. The schematic of the LED-sensor with a list of parts is illustrated in Fig. 1. The components with the lowest temperature coefficient available were used. The cost of one LED-sensor including all parts was approximately 150$.

2.2.2. Selecting LEDs

We selected two bands of LEDs that include red (peak sensitivity: 646 nm, full width half maximum (FWHM): 56 nm, field of view (FOV): 120°, model: Lumex SSL-LX5093SRD, Palatine, IL) and near-infrared (peak sensitivity: 843 nm, FWHM: 72 nm, FOV: 80°, model: Fairchild F5E3, San Jose, CA). The spectral, thermal and angular characterizations of the light emitting diodes as detectors were carried out at the Center for Applied Science and Technology of the National Autonomous University of Mexico (Rosete-Aguilar et al., 2003; Ruiz-Mercado, 2005) and at the National Metrology Center in Querearo, Mexico (Arroyo Camacho et al., 2004). Among the available wavebands in off-the-shelf LEDs, we selected this pair based on their spectral response, seeking to avoid atmospheric absorption bands and to match as close as possible the red (620–670 nm) and NIR (841–876 nm) spectral bands of the Moderate Resolution Imaging Spectroradiometer (MODIS) which are used to calculate MODIS normalized vegetation index (NDVI) (Huete et al., 2002; Tucker, 1979):

$$\mathrm{NDVI} = \frac{\rho_{\mathrm{NIR}} - \rho_{\mathrm{RED}}}{\rho_{\mathrm{NIR}} + \rho_{\mathrm{RED}}} \quad (1)$$

where ρ_{NIR} and ρ_{RED} are reflectance of NIR and red bands, respectively.

2.2.3. Description of the sensor head

The upward facing sensor head was constructed from 6.35 mm (1/4 in.) and 9.53 mm (3/8 in.) wide rings cut from 50.8 mm (2 in.) OD aluminum pipe with 6.35 mm (1/4 in.) thick wall. These rings sandwiched a circular plate 1.59 mm (1/16 in.) thick cut from round aluminum bar. The 6.35 mm (1/4 in.) ring was placed above the plate and the 9.53 mm (3/8 in.) ring below the plate. A 50.8 mm (2 in.) diameter disk of 0.79 mm (1/32 in.) thick Teflon sheet (Teflon®, DuPont, Wilmington, DE, USA) was placed on the top to diffuse the light to reduce the directional characteristics

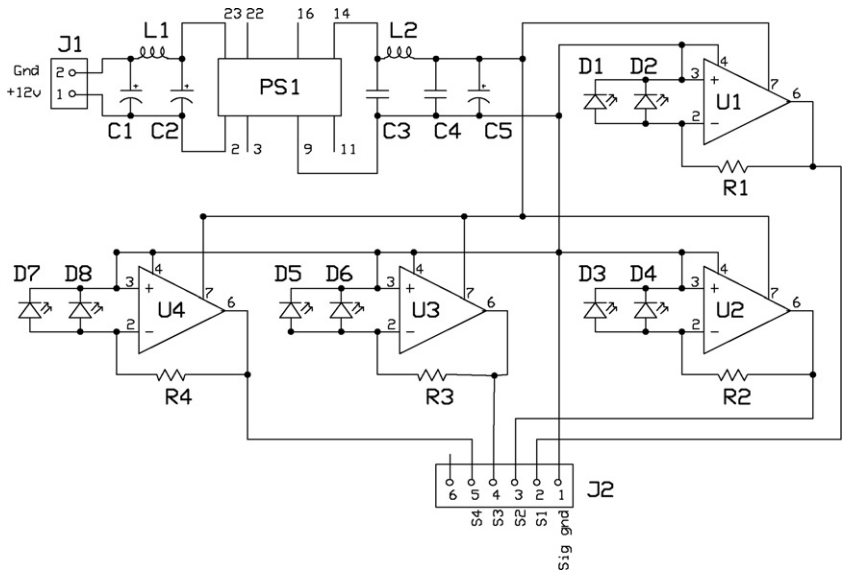

Fig. 1. Schematic of LED NDVI sensor. R1 = 150 kΩ, 0.1% 10 ppm/C; R2 = 100 kΩ, 0.1%, 10 ppm/C; R3 = 1 MΩ, 0.1%, 10 ppm/C; R4 = 499 kΩ, 0.1%, 10 ppm/C; D1, D2, D5, D6 = Lumex Inc. smf-hm1530srd-509; D3, D4, D7, D8 = fairchild semiconductor, F5E1; C1, C2 = 4.7 μF, electrolytic; C3, C4 = 0.01 μF, ceramic; C5 = 4.7 μF, tantalum; L1, L2 = KOASpeer, 2.2 μH, LPC4045LTED2R2M; U1, U2, U3, U4 = linear technology, LTC1050; PS1 = CalEx, 24D12.250HW. D1–D4 are incoming radiation collectors and D5–D8 are reflected radiation collectors.

of the LEDs. Thus, the full viewing angle of the LED-sensor for both upward and downward was approximately 180°. Four LEDs (two red and two NIR) were mounted through the plate and affixed to the plate with a small circuit board using a central 6-32 screw. The whole assembly was bolted to a mounting arm using four 6-32 bolts running vertically though the Aluminum and Teflon parts at equal intervals around the diameter of the head. The downward sensor head was constructed similarly but oriented in the opposite direction. The outside was painted white to seal joints and reduce solar heating. Fig. 2 shows the sensor head.

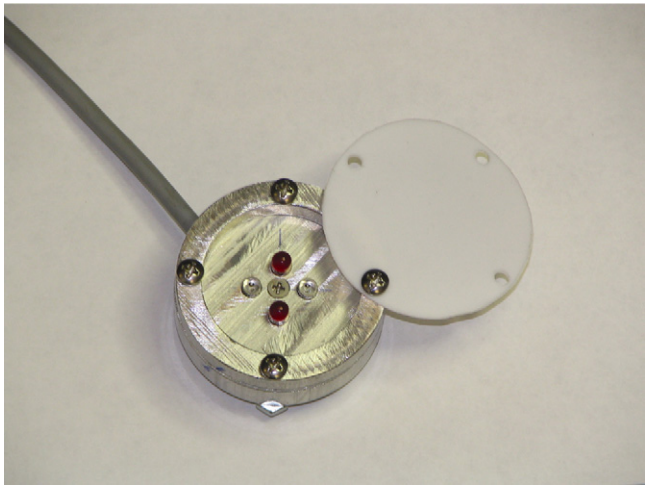

Fig. 2. LED-spectrometer head. The two red sensors are LEDs in the red wavelength, and the two colorless sensors are LEDs in the NIR wavelength. The white cover is Teflon to diffuse the incoming light. (For interpretation of the references to color in this figure legend, the reader is referred to the web version of the article.)

2.3. Testing the LED-sensor

2.3.1. Comparing LED-sensor with hyper-spectrometer in the lab

A laboratory experiment was conducted to compare the response of both the upward and downward red and NIR LED-sensor faces with a hand-held spectrometer (USB2000, Ocean Optics Inc., Dunedin, FL), which had been calibrated against a National Institute of Standards and Technology (NIST) traceable, tungsten halogen light source. The two LED-sensor faces and spectrometer head were placed together as closely as possible and exposed to a 100 W incandescent bulb with reflective hood. The light source started at 40 cm above the sensor faces and was moved away in 22 steps of 2.54 cm. The output of the spectrometer (counts, 250 ms integration) was sub-sampled using the normalized response spectrums of the LEDs and then compared to the output of the LEDs (mV). This test showed high linear relation between the LEDs and the hyper-spectrometer with the LEDs having R^2 values greater than 0.94 for the red and greater than 0.99 for the NIR (Fig. 3). These results are in agreement with previous laboratory studies of the linear response of similar LED radiometers (Velasco-Segura, 2005; Velasco-Segura and Rosete-Aguilar, 2003) that have shown the non-linearity of such systems to be well under 1% and to be comparable to identical circuits using regular silicon photodiodes as detectors.

2.3.2. Field comparison of spectral reflectance between LED-sensor and hyper-spectrometer

For field application, we installed the LED-sensor on a horizontal boom 3 m above the ground surface. A data logger (Model CR23X, Campbell Sci., Inc., CSI, Logan Utah) sampled irradiance from the four channels every 10 s and stored half-hour mean values.

To evaluate the stability of the LED-sensor, we regularly measured hyper-spectral reflectance (range: 400–900 nm, FWHM: 1.3 nm) at the canopy scale with the hand-held spectrometer (USB2000, Ocean Optics Inc., Dunedin, FL). The spectrometer was mounted on a portable tripod with an attached aluminum boom, connected to a 2 m fiber optic transmitter and a cosine-corrector (Teflon®) with a 180° FOV. Measurement height above the grass canopy was kept at 1 m. Vegetation spectral reflectance was obtained by measuring both incoming and reflected irradiance spectra with the same spectrometer in sequence, using the same

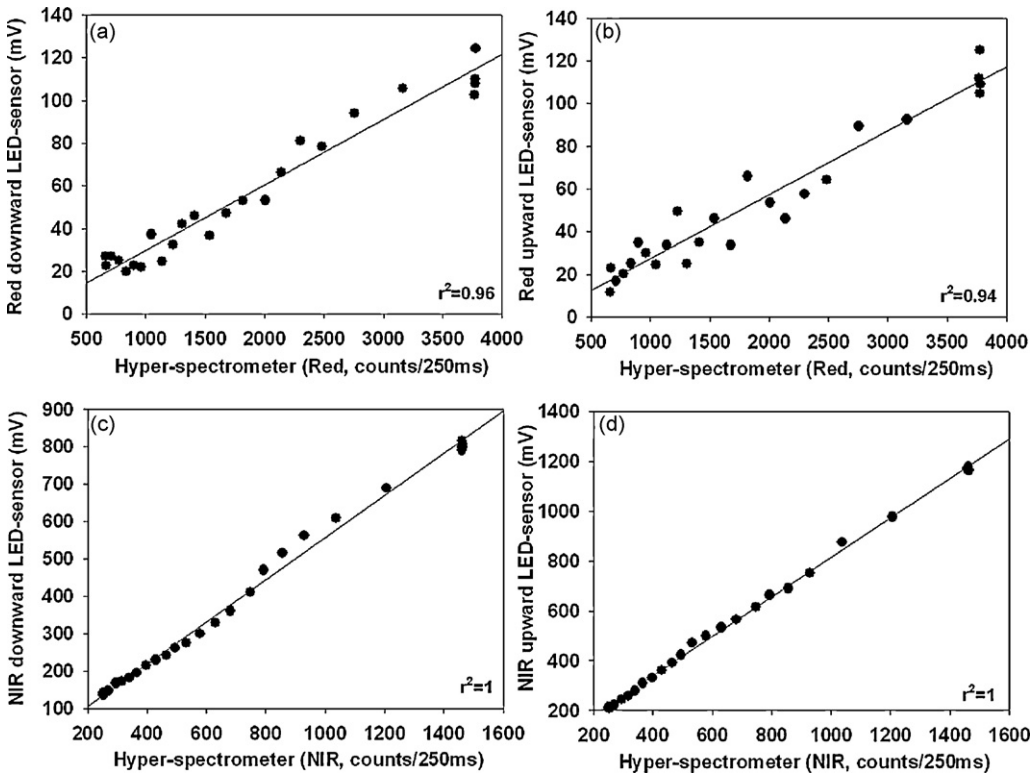

Fig. 3. Scatterplots between hyper-spectrometer and LED-sensor outputs tested in the lab with a stable light source. Peak and full-width-half-maximum (FWHM) of red and NIR LEDs were 646 (56) and 843 (72) nm, respectively (parenthesis values indicate FWHM). (a) Red waveband for downward red-LED and hyper-spectrometer. (b) Red waveband for upward red-LED and hyper-spectrometer. (c) NIR waveband for downward NIR-LED and hyper-spectrometer. (d) NIR waveband for upward NIR-LED and hyper-spectrometer.

integration time and instrument configuration. We randomly sampled at least three points within a 5-m radius of the LED-sensor and then averaged the spectral reflectance of the samples. The output of the hand-held spectrometer was sub-sampled to match the red and NIR bands in the LEDs (Fig. 4a). We found that there has been no significant drift in the two bands by comparing the mean ± 95% confidence intervals of the slopes for the 3.5 years ($p > 0.05$, linear regression forced to pass through the origin) (Fig. 4). Finally, we corrected the raw reflectance of the LED-sensor by dividing by 1.33 (red band, the slope of Fig. 4a) and 1.68 (NIR band, the slope of Fig. 4b).

2.3.3. Response of red and NIR LEDs to different solar zenith angles

To test the cosine response of LED-sensor equipped with Teflon diffuser, we compared the relative response of red and NIR LEDs (upward direction) with the ideal cosine curve (Fig. 5). The difference between the LEDs and the ideal cosine curve was less than 20% within 60° of solar zenith angle and was ~30% at 70° of solar zenith angle. This response is comparable with the photodiode-based spectrometer (Garrity et al., 2010).

2.3.4. Temperature sensitivity of LED-sensor

We quantified the temperature sensitivity of the LED-sensor using the following equation (Arroyo Camacho et al., 2004):

$$C_{\text{T-rel}} = \frac{s(T_2) - s(T_1)}{(s(T_2) + s(T_1))/2} \cdot \frac{1}{T_2 - T_1} \quad (2)$$

where $C_{\text{T-rel}}$ is the temperature coefficient ($1\,^{\circ}\text{C}^{-1}$), $s(T)$ is signal at temperature T. This sensitivity test was carried out at the Center for Applied Science and Technology of the National Autonomous University of Mexico (Arroyo Camacho et al., 2004; Ruiz-Mercado, 2005). The $C_{\text{T-rel}}$ of the LED Red and NIR at their peak wavelengths (646 and 843 nm for red and NIR, respectively) were $0.3\%\,^{\circ}\text{C}^{-1}$ and $-0.02\%\,^{\circ}\text{C}^{-1}$, respectively in the range of 20–52 °C. We installed thermocouples in the upward and downward faces of the LED-sensor in the field and have collected the LED-sensor temperature data. There was almost no temperature difference between the two faces (RMSE = 0.16 °C) and midday temperatures ranged from 7 to 46 °C over the 3.5 years. We tested the effects of LED temperature on the red and NIR reflectance and NDVI. Among 1-month data during the summer dry season when the grass is dead (DOY 210–240 in the 2006 year), we only selected the data for clear sky days and fixed solar zenith angle (30°). The volumetric soil moisture at the 5-cm depth ranged 3.3–3.5% during this period. The LED temperature varied from 27 to 40 °C, but the red, NIR reflectance and NIR did not change much. The red reflectance ranged 0.17–0.18, the NIR reflectance varied 0.29–0.31, and NDVI ranged 0.25–0.29. The slopes of the three figures showed no significant difference from zero (linear regression, $p = 0.9$, 0.4, and 0.2 for red, NIR and NDVI, respectively). It should be noted that since the LEDs exhibit a very linear thermal response within these temperature ranges (Arroyo Camacho et al., 2004), the temperature sensitivity of LED-sensor is largely removed because we used ratio of upward and downward LEDs, which had almost identical temperature.

3. Ancillary measurements to test LED-sensor for monitoring ecosystem structure, function and metabolism

We used an eddy covariance system to measure net ecosystem carbon exchange (NEE). Ecosystem respiration was quantified

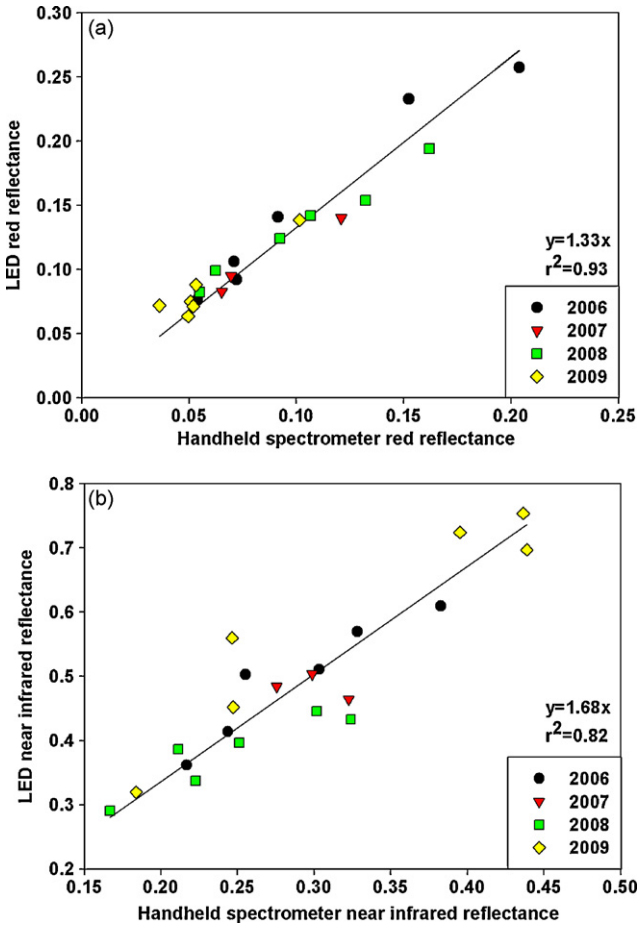

Fig. 4. Inter-comparison of reflectance between LED-sensor and hyperspectrometer for (a) red and (b) NIR. The raw LED-sensor reflectance was corrected by dividing by the slopes (see Section 2.3.2). (For interpretation of the references to color in this figure legend, the reader is referred to the web version of the article.)

based on the regression models between nighttime NEE and soil temperature at 4 cm depth for measurements under high turbulence condition (friction velocity > 0.1 m s^{-1}). Then grass gross photosynthesis was quantified as the difference between NEE and ecosystem respiration (Ma et al., 2007). We regularly measured grass LAI during the active period by harvesting four sample plots (0.25 m × 0.25 m). Leaf nitrogen content of grass (% of dry weight) was determined with a plant chemical analyzer at the Center for Stable Isotope Biogeochemistry, UC Berkeley. We recorded grass green-up and senescence dates when 90% of grass community was either alive or dead, respectively, based on weekly to bi-weekly visual inspections (Table 1).

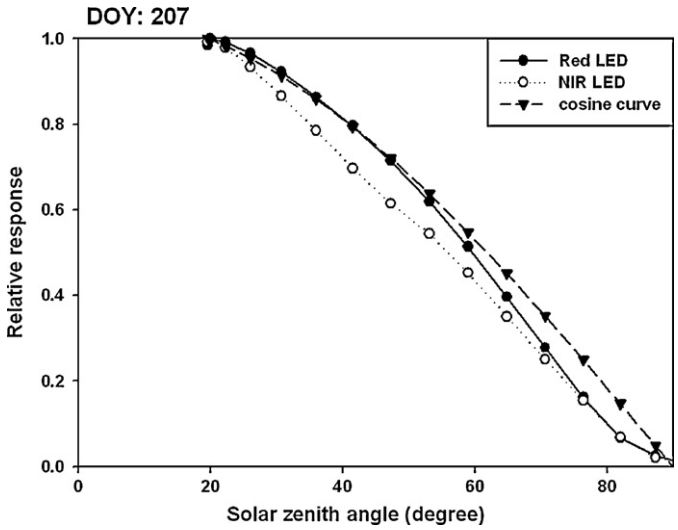

Fig. 5. Relative response of the red and NIR LEDs compared with the ideal cosine curve. The data was taken in DOY207, 2007.

4. Application of LED-sensor

4.1. Effects of the solar zenith angles on the red, NIR reflectance and NDVI of the LED-sensor

The dependence of the spectral reflectance on the solar zenith angle is crucial to understand seasonal variations of spectral reflectance and vegetation indices. For example, Sims et al. (2006) reported that the diurnal variation of NDVI was larger than the seasonal variation of NDVI in a chaparral site, and the seasonal variations of NDVI in the local noon and solar zenith angle at 60° were out-of-phase and showed different magnitudes. Thus we investigated the effect of solar zenith angle on the spectral reflectance and NDVI at both diurnal and seasonal scales. In our study site, we found that diurnal variation in the red reflectance was less than 0.15. The NIR reflectance showed greater diurnal variation over the course of the year up to 0.3 (Fig. 7b). However, the NDVI did not show pronounced diurnal variation (Fig. 7c) contrary to the Sims et al. (2006). We presume that the land surface heterogeneity would explain the discrepancy. The vegetation distribution was clumped and half of the surface was bare soil at the study site of Sims et al. (2006) (see Fig. 8 in Gamon et al., 2006a) whereas the grass community covered most land surface in the current study site. Next, we compared the NDVI, red and NIR reflectance between the local noon and fixed solar zenith angle at 60° in the year of 2007 (Fig. 7d–f). Both red and NIR reflectance showed large difference in their magnitudes between the two cases in the summer when the grass is dead and solar zenith angle is much lower than 60°. However, the two cases were in-phase

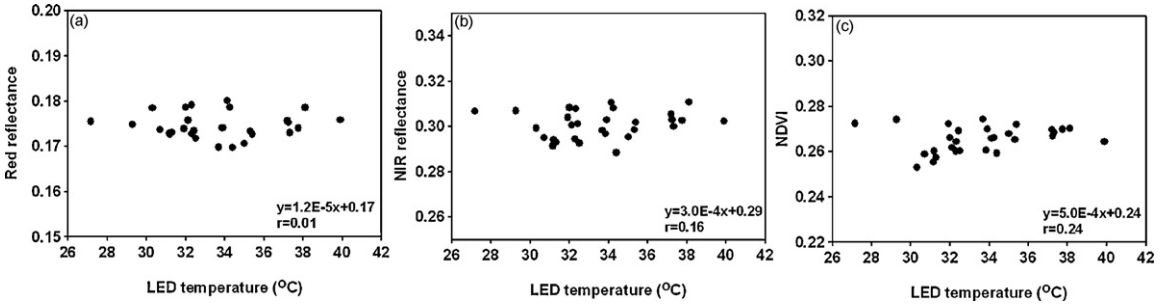

Fig. 6. Scatterplots between LED temperature and (a) red reflectance, (b) NIR reflectance, and (c) NDVI during the summer dry season (DOY 210–240 in the 2006 year) when the grass is dead. During this period, we selected data for the fixed solar zenith angle (60°) and clear sky days.

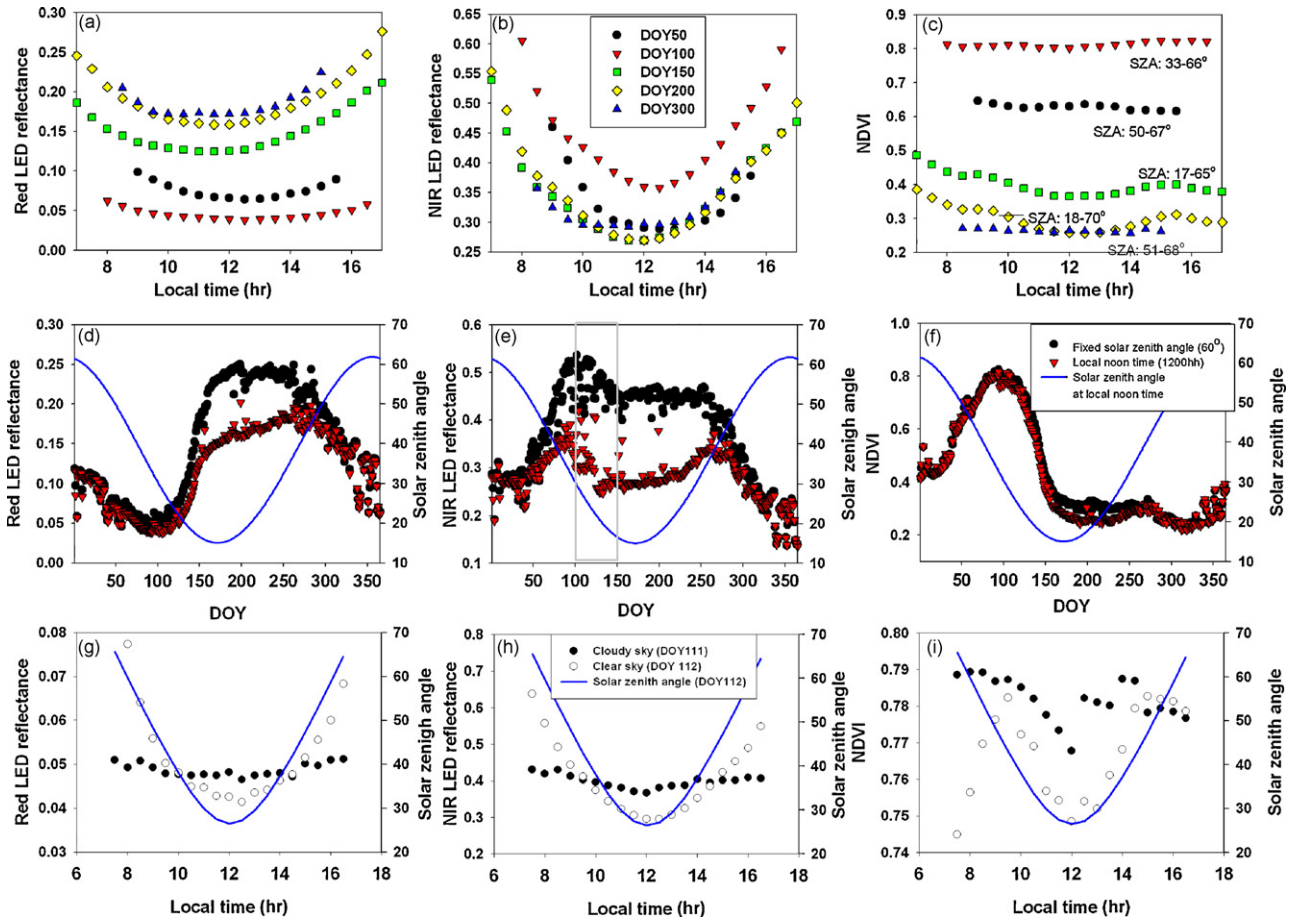

Fig. 7. (a)–(c) Diurnal variation of red reflectance (a), NIR reflectance (b), and NDVI (c) at five dates. DOY50 (green-up), DOY100 (peak green), DOY150 (green-down), DOY200 (dead grass), DOY300 (leaf-on). (d)–(f) Daily variation of red reflectance (d), NIR reflectance (e) and NDVI (f). The values were calculated at fixed solar zenith angle (60°) and local noon time. (g)–(i) Comparison of red reflectance, NIR reflectance and NDVI derived from the LED-spectrometer between cloudy (DOY111) and clear (DOY 112) sky days. (For interpretation of the references to color in this figure legend, the reader is referred to the web version of the article.)

and shared important transition points (e.g. peak timings, reflection points). Again, the NDVI was not sensitive to the solar zenith angle and showed similar seasonal pattern between the two cases (Fig. 7f).

We tested the impact of sky condition on the spectral reflectance and NDVI (Fig. 7g–i), which could help better interpret their seasonal variation. As expected, both red and NIR reflectance were strongly related with the solar zenith angle only on the clear sky day (DOY 112), not on the cloudy sky day (DOY111). Overall, the NDVI showed very small diurnal variation (only 6% variation of the mean value) and it was slightly higher for the cloudy day than the clear sky day (Fig. 7i). It is notable that the clear and cloudy lines intersected at ~50° of solar zenith angle (Fig. 7g and h), indicating that spectral reflectance of cloudy condition could be higher or lower than that of clear sky depending on the solar zenith angle. For example, in the grey box of Fig. 7e, the deviated points from the general pattern were cloudy sky days. For those cloudy days, the local noon data (20–40° of solar zenith angle in this period) and the data at the 60° of solar zenith angle presented the opposite signs from the general pattern because of the solar zenith angle. The LED-sensor allows us to investigate the effect of sky condition on the spectral reflectance which is hard to obtain from the satellite or periodic manual sampling. We conclude that the red and NIR reflectance are moderately to strongly related with solar zenith angles, but the NDVI is not sensitive to the solar zenith angle in the study site.

4.2. Seasonal and interannual variation of spectral reflectance

The red and NIR reflectance at local noon showed pronounced seasonal and interannual variability (Fig. 8b). The NDVI ranged from 0.2 to 0.85 as LAI varied from near 0 to 2.5, thus the LED-sensor detected a broad ranges in vegetation condition. Healthy green vegetation absorbs most of the incident visible radiation, particularly in the red portion of the spectrum, and reflects and transmits most of the incident NIR. Consequently, the temporal variation of the red and NIR reflectance was mirrored when grasses were active. Notably, the first and second rain pulses after the prolonged summer drought caused an abrupt decrease of the spectral reflectance of both wavelength bands.

The LED-sensor was able to track interannual variations in canopy structure as well. We observed the lowest LAI (Fig. 8c) and canopy photosynthesis (Fig. 9b) in 2008, which recorded the lowest rainfall among the 4 years (Fig. 8a). The NDVI signal agreed with those observations by showing the lowest peak NDVI value in 2008 (Fig. 8c). The NIR reflectance in the 2008 spring was the lowest among the 4-year springs, presumably because low green LAI reduces NIR reflectance in dark background (Gao et al., 2000; Hollinger et al., 2009; Sellers, 1985) (Fig. 8c). We found that both red and NIR reflectance during the dry summer 2008 was significantly lower than the other years (DOY 200–260, $p < 0.05$, Tukey–Kramer test). Dead grass is very bright (higher reflectance) compared to the darker background soil. Thus we assumed that less grass produc-

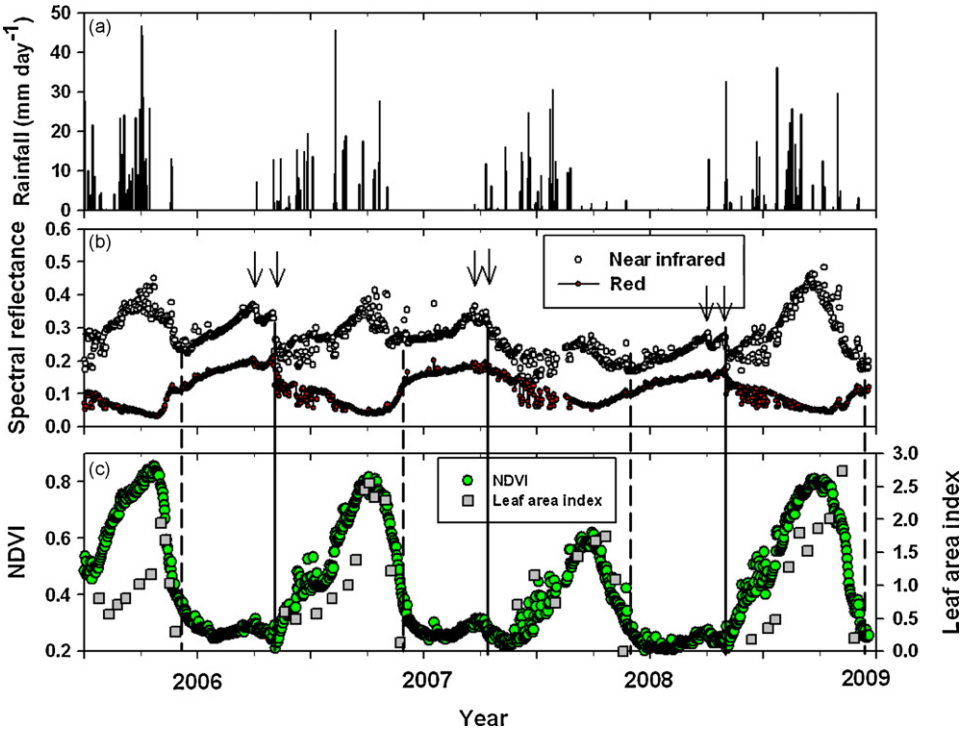

Fig. 8. (a) Time series of daily rainfall. (b) Red and near-infrared reflectance (local noon) of LED-spectrometer from 2006 January to 2009 June. Vertical arrows indicate the first and second rainfalls in the transition between dry and wet seasons. Horizontal arrows indicate an example of the cloudy condition. (c) Time series of LEDs derived NDVI (midday) and leaf area index (weekly to bi-weekly when grass is alive) measured using harvest method. All LEDs reflectance was calculated at local noon time measurements. The vertical dashed (solid) lines indicate the dates of grass offset (onset) (see Section 4.2 for details). (For interpretation of the references to color in this figure legend, the reader is referred to the web version of the article.)

tion in the previous growing season led to less dead grass biomass, higher proportion of the darker background soil within the FOV of the LED-sensor, thus lower reflectance at the red and NIR bands (Middleton, 1991). The previous studies conducted at the same site showed that maximum grass LAI is very sensitive to the rainfall amount in the spring (Ma et al., 2007; Ryu et al., 2008). Thus the spring rainfall would be the main driver to control the carbon sequestration in the spring and the land surface radiation balance during the summer. Continuous monitoring of the vegetation spectral reflectance will be useful to test this hypothesis. The above analysis and interpretations are valid even using the red and NIR reflectance data at 60° of solar zenith angle.

4.3. Extracting key phenological events of grass community

LED-based reflectance clearly showed the phenological cycles of the grass community (Fig. 8b and c). We visually identified the dates of leaf-on when red (NIR) reflectance abruptly decreases (increases) after autumn rainfall (vertically solid lines in Fig. 8a and b), which indicates the onset of photosynthesis. They showed low absolute mean bias error (5.3 ± 0.4 days, mean ± standard error) against weekly to bi-weekly field observation (Table 1). We determined the leaf-off dates as averages of when the NIR reflectance is at its minimum and the slope of the red reflectance abruptly changes (vertically dashed lines in Fig. 8b and c), indicating that the grass LAI is at a minimum. The calculated leaf-off dates also showed low absolute mean bias error (4.2 ± 1.6 days) against field observation. Leaf-on and leaf-off dates, derived from the LED-sensor, defined the seasonality of LAI values well (Fig. 8c). Strengths of using the LED-sensor for phenological research include high temporal resolution and general applicability regardless of weather conditions except for when the foreoptics are wet. Satellite-based phenology studies have coarse temporal resolutions, and thus the interpolation of a time series into daily resolution remains a critical issue (Morisette et al., 2009; White et al., 2009).

Table 1
Leaf-on and leaf-off dates recorded from field observation (weekly to bi-weekly) and LED-sensor.

	Leaf-on dates (day of year)		Leaf-off dates (day of year)	
	Observation	LED-sensor	Observation	LED-sensor
2005–2006			154	155
2006–2007	312	307	152	158
2007–2008	289	283	146	149
2008–2009	308	303	147	154
Mean	303	297.7	149.8	154

4.4. Investigating seasonality of canopy photosynthesis

Canopy photosynthesis is an essential variable to understand the interactions between ecosystem and climate, yet measuring canopy photosynthesis has been limited due to expensive instrument systems (e.g. eddy covariance method Baldocchi, 2008) or labor-intensive ecosystem inventory (Clark et al., 2001). Alternatively, the remote sensing community has used normalized difference vegetation indices widely to infer canopy photosynthesis (Fung et al., 1987; Gamon et al., 1992; Gitelson et al., 2003; Sellers, 1985); remotely sensed vegetation index, like NDVI, has to be used with caution because NDVI is known to saturated where LAI is greater than 3 (Sellers, 1985). For the California grassland, we found that NDVI values, derived from the LED-sensor, explained 91% of variance in the canopy photosynthesis over 3.5-year (Fig. 9b). At our study site, LAI is typically less than 3 and most canopy photosynthesis happens in the wet period. Consequently, NDVI is a good indicator to estimate canopy photosynthesis of annual grasslands as reported by Gamon et al. (1995).

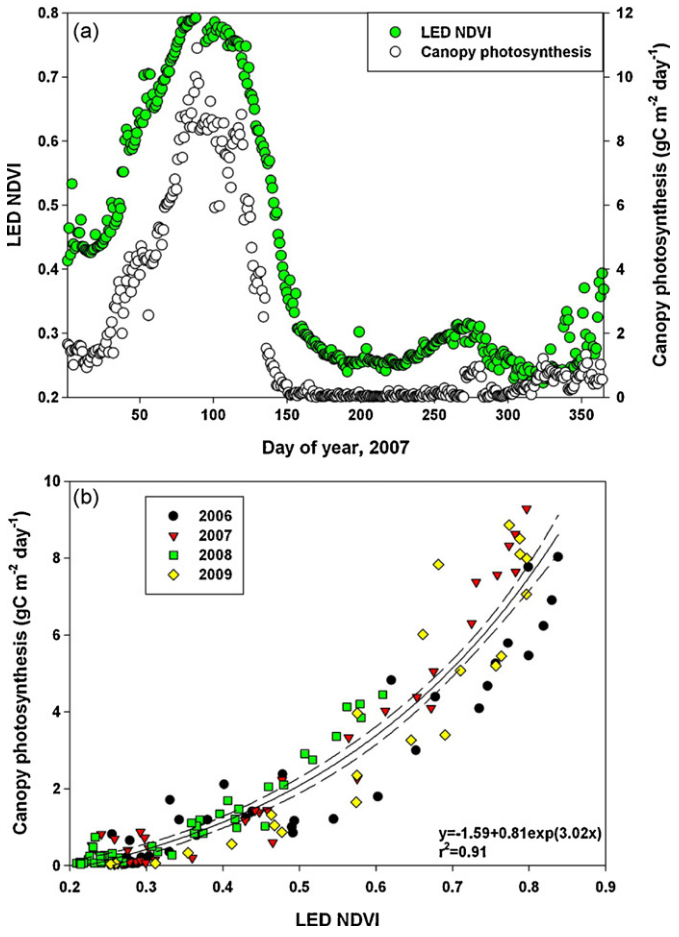

Fig. 9. (a) Time series of daily canopy photosynthesis from eddy flux tower and midday LEDs derived NDVI in 2007. (b) Scatter plot between 8-day mean of midday LEDs derived NDVI and 8-day mean canopy photosynthesis from 2006 January to 2009 July. Dashed line indicates 95% confidence interval on the linear regression (solid line).

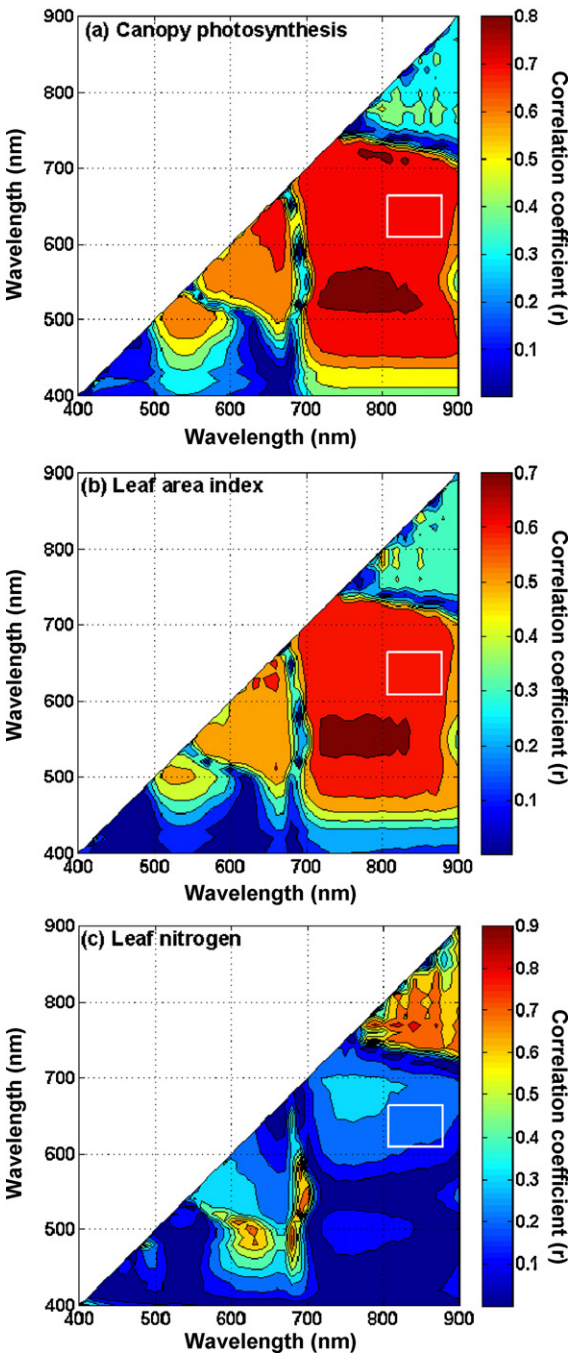

Fig. 10. Contour maps of correlation coefficient (r) between normalized difference spectral indices using two wavelengths (x and y axis) and (a) canopy photosynthesis ($n = 33$), (b) leaf area index ($n = 33$), and (c) leaf nitrogen ($n = 10$). White rectangular box indicates the spectral region of LEDs derived NDVI instrument.

An exponential relation between NDVI and canopy photosynthesis is notable over the course of the growing season (November–May) (Fig. 9b). This non-linearity occurs because canopy photosynthesis is a multiplicative function of two processes upon which NDVI could be correlated; these are the fraction of absorbed PAR (fPAR) (Goward and Huemmrich, 1992; Sellers, 1985; Sims et al., 2006) and light use efficiency (Nakaji et al., 2008; Sims et al., 2006). Consequently, the increase in the first derivative of the exponential curve with NDVI is a reflection of the combined increase in leaf area index, fPAR and light use efficiency during the active growth period when soil moisture is ample. In contrast, the period when NDVI is low corresponds with the severe drought period when leaf area index, fPAR and light use efficiency are low. The saturation of NDVI with increase of LAI is unlikely substantial because the maximum LAI in the study site was ~2.5 where NDVI is not saturated (Huete et al., 2002; Sellers, 1985). We conclude that the exponential relationship between NDVI and canopy photosynthesis may be an inherent property of seasonally droughted grassland ecosystems when LAI is less than 3.

4.5. Exploring optimal LED wavelengths for improved monitoring of ecosystem structure and metabolism

To explore the potential of other spectral regions to better monitor canopy photosynthesis, LAI and leaf nitrogen related with 4th scientific question raised in the introduction, we compute a continuum of normalized difference spectral indices (i.e. Eq. (1) using two different wavebands) (Inoue et al., 2008; le Maire et al., 2008), which were measured with the hand-held hyper-spectral radiometer, and correlate these indices with independent variables like canopy photosynthesis. The area of wavelengths that the LED-sensor covers (white rectangular box in Fig. 10(a)–(c)) did not show the highest correlation with these three variables. We found that a normalized difference spectral index that combines green (~550 nm) and NIR (730–830 nm) showed the highest correlation with canopy photosynthesis (Fig. 10a) and LAI (Fig. 10b). This spectral region can be covered by commercially available LEDs so we have the possibility to redesign the LED-spectrometer by target-

ing this high correlation spot. We found that leaf nitrogen showed high correlation with specific NIR bands (800–850 and ~780 nm) or between the red edge (~700 nm) and blue (~480 nm) or green (~520 and ~580 nm) bands. The off-the-shelf LEDs that can detect the NIR region are available, but the LEDs are not suitable to monitor the red-edge region because of its very narrow waveband. We conclude that a wide range of wavebands in the off-the-shelf LEDs allows us to target the high correlation spectral regions related with canopy photosynthesis, LAI and N. We also note that LED-sensor has limitation for monitoring very narrow waveband (e.g. the red-edge region).

4.6. Broader implications

Based on a variety of spectral wavebands, inexpensive price and reliable performance, the LED-sensor has the potential for wide-spread application on many remote sensing and ecological topics. Firstly, the LED-sensor has the potential to replace expensive four-bands radiometer (Fensholt and Sandholt, 2005) and be deployed widely among a number of long-term ecosystem monitoring programs like the global spectral reflectance network (SpecNet) (Gamon et al., 2006b), Long Term Ecological Research Network (http://www.lternet.edu/), National Ecological Observatory Network (http://www.neoninc.org/), global eddy flux tower network-FLUXNET (Baldocchi et al., 2001). Secondly, deployment of the LED-sensor gives investigators the potential to infer ecosystem metabolism, structure and function in treatment plots that may be too small for application of the eddy covariance method or in plots where repeated sample is too expensive, such as in Free-Air Carbon Dioxide Enrichment (FACE) studies (Norby et al., 2005), biodiversity (Tilman et al., 2001) and biofuel (Heaton et al., 2008) field trials and ecosystem manipulation experiments. Finally, the LED-sensor could be instrumental in the educational realm as well. Students have used an LED-sensor to monitor atmospheric turbidity in the Global Learning and Observations to Benefit the Environment Program (Mims, 1999). Here, we recommend that students use two sets of LED-sensors (upward and downward), to learn how vegetation reflectance changes with different surface properties.

5. Summary and conclusions

To link remote sensing with ecosystem fluxes, there are pressing needs to develop inexpensive but reliable spectrometers. In this study, we reported on a novel, inexpensive spectral sensor equipped with LEDs. The lab and field tests revealed that the LED-sensor showed highly linear relation with the hyperspectral spectroradiometer (Fig. 3) and marginal sensitivity to temperature (Eq. (2), Fig. 6). Based on the 3.5 years of data from an annual grassland, we found that the LED-sensor is able to monitor daily to interannual variations of vegetation spectral reflectances. The continuous measurements of spectral reflectance enabled us to track the ecosystem phenology (5.3 and 4.2 days of the mean bias errors at leaf-on and leaf-off dates, respectively) and estimate canopy photosynthesis ($R^2 = 0.91$). The LED-sensor is a cost-effective solution to monitor vegetation structure and metabolism variables with high flexibility in the wavebands selection than most other spectrometers. We believe that the LED-sensor can be used in a variety of ecological applications.

Acknowledgements

Youngryel Ryu was supported by NASA Headquarters under the NASA Earth and Space Science Fellowship Program (NNX08AU25H) and the Berkeley Water Center/Microsoft eScience project. Drs. Josep Peñuelas and Hideki Kobayashi provided constructive comments. We thank Martha Rosete-Aguilar, Roberto Velasco-Segura, and Matias Arroyo Chamacho for their assistance in characterizing LED-sensor. We thank Jaclyn Hatala for proofreading the manuscript. This research was conducted at the site that is a member of the AmeriFlux and Fluxnet networks and supported in part by the Office of Science (BER), the U.S. Department of Energy (DE-FG02-03ER63638). Two anonymous reviewers and the editor, Dr. John Gash, gave constructive comments which improved the quality of this manuscript substantially.

References

Acharya, Y.B., Jayaraman, A., Ramachandran, S., Subbaraya, B.H., 1995. Compact light-omitting-diode sun photometer for atmospheric optical depth measurements. Appl. Opt. 34 (7), 1209–1214.

Arroyo Camacho, M.L., Schmid, W.A., Molina Vazquez, J.C., Rosete Aguilar, M., Ruiz Mercado, I., 2004. Characterization of the spectral responses of LEDs as optical detectors at the range between 20 °C and 75 °C. In: Meteorology Symposium, Querétaro, Mexico.

Asner, G.P., Martin, R.E., 2009. Airborne spectranomics: mapping canopy chemical and taxonomic diversity in tropical forests. Front. Ecol. Environ. 7 (5), 269–276.

Baldocchi, D.D., 2008. 'Breathing' of the terrestrial biosphere: lessons learned from a global network of carbon dioxide flux measurement systems. Aust. J. Bot. 56, 1–26.

Baldocchi, D., Valentini, R., Running, S., Oechel, W., Dahlman, R., 1996. Strategies for measuring and modelling carbon dioxide and water vapour fluxes over terrestrial ecosystems. Global Change Biol. 2 (3), 159–168.

Baldocchi, D., Falge, E., Gu, L.H., Olson, R., Hollinger, D., Running, S., Anthoni, P., Bernhofer, C., Davis, K., Evans, R., Fuentes, J., Goldstein, A., Katul, G., Law, B., Lee, X.H., Malhi, Y., Meyers, T., Munger, W., Oechel, W., Paw, U., K.T. Pilegaard, K., Schmid, H.P., Valentini, R., Verma, S., Vesala, T., Wilson, K., Wofsy, S., 2001. FLUXNET: A new tool to study the temporal and spatial variability of ecosystem-scale carbon dioxide, water vapor, and energy flux densities. Bull. Am. Meteorol. Soc. 82 (11), 2415–2434.

Barr, A.G., Black, T.A., Hogg, E.H., Kljun, N., Morgenstern, K., Nesic, Z., 2004. Interannual variability in the leaf area index of a boreal aspen-hazelnut forest in relation to net ecosystem production. Agric. For. Meteorol. 126 (3–4), 237–255.

Black, T.A., Chen, W.J., Barr, A.G., Arain, M.A., Chen, Z., Nesic, Z., Hogg, E.H., Neumann, H.H., Yang, P.C., 2000. Increased carbon sequestration by a boreal deciduous forest in years with a warm spring. Geophys. Res. Lett. 27 (9), 1271–1274.

Brooks, D.R., Mims, F.M., 2001. Development of an inexpensive handheld LED-based Sun photometer for the GLOBE program. J. Geophys. Res. 106 (D5), 4733–4740.

Carrara, A., Kowalski, A.S., Neirynck, J., Janssens, I.A., Yuste, J.C., Ceulemans, R., 2003. Net ecosystem CO_2 exchange of mixed forest in Belgium over 5 years. Agric. For. Meteorol. 119 (3–4), 209–227.

Clark, D.A., Brown, S., Kicklighter, D.W., Chambers, J.Q., Thomlinson, J.R., Ni, J., 2001. Measuring net primary production in forests: concepts and field methods. Ecol. Appl. 11 (2), 356–370.

Fensholt, R., Sandholt, I., 2005. Evaluation of MODIS and NOAA AVHRR vegetation indices with in situ measurements in a semi-arid environment. Int. J. Remote Sens. 26 (12), 2561–2594.

Fung, I.Y., Tucker, C.J., Prentice, K.C., 1987. Application of advanced very high resolution radiometer vegetation index to study atmosphere–biosphere exchange of CO_2. J. Geophys. Res. 92 (D3), 2999–3015.

Gamon, J.A., Penuelas, J., Field, C.B., 1992. A narrow-waveband spectral index that tracks diurnal changes in photosynthetic efficiency. Remote Sens. Environ. 41 (1), 35–44.

Gamon, J.A., Field, C.B., Goulden, M.L., Griffin, K.L., Hartley, A.E., Joel, G., Penuelas, J., Valentini, R., 1995. Relationships between NDVI, canopy structure, and photosynthesis in three Californian vegetation types. Ecol. Appl. 5 (1), 28–41.

Gamon, J.A., Cheng, Y., Claudio, H., MacKinney, L., Sims, D.A., 2006a. A mobile tram system for systematic sampling of ecosystem optical properties. Remote Sens. Environ. 103 (3), 246–254.

Gamon, J.A., Rahman, A.F., Dungan, J.L., Schildhauer, M., Huemmrich, K.F., 2006b. Spectral Network (SpecNet)—what is it and why do we need it? Remote Sens. Environ. 103 (3), 227–235.

Gao, X., Huete, A.R., Ni, W., Miura, T., 2000. Optical–biophysical relationships of vegetation spectra without background contamination. Remote Sens. Environ. 74, 609–620.

Garrity, S.R., Vierling, L.A., Bickford, K., 2010. A simple filtered photodiode instrument for continuous measurement of narrowband NDVI and PRI over vegetated canopies. Agric. For. Meteorol. 150 (3), 489–496.

Gitelson, A.A., Verma, S.B., Vina, A., Rundquist, D.C., Keydan, G., Leavitt, B., Arkebauer, T.J., Burba, G.G., Suyker, A.E., 2003. Novel technique for remote estimation of CO_2 flux in maize. Geophys. Res. Lett. 30 (9), 1486, doi:10.1029/2002GL016543.

Goward, S.N., Huemmrich, K.F., 1992. Vegetation canopy PAR absorptance and the normalized difference vegetation index: an assessment using the SAIL model. Remote Sens. Environ. 39 (2), 119–140.

Heaton, E.A., Dohleman, F.G., Long, S.P., 2008. Meeting US biofuel goals with less land: the potential of Miscanthus. Global Change Biol. 14 (9), 2000–2014.

Hilker, T., Coops, N.C., Nesic, Z., Wulder, M.A., Black, A.T., 2007. Instrumentation and approach for unattended year round tower based measurements of spectral reflectance. Comput. Electron. Agric. 56 (1), 72–84.
Hollinger, D.Y., Ollinger, S.V., Richardson, A.D., Meyers, T.P., Dail, D.B., Martin, M.E., Scott, N.A., Arkebauer, T.J., Baldocchi, D.D., Clark, K.L., Curtis, P.S., Davis, K.J., Desai, A.R., Dragoni, D., Goulden, M.L., Gu, L., Katul, G.G., Pallardy, S.G., PawU, K.T., Schmid, H.P., Stoy, P.C., Suyker, A.E., Verma, S.B., 2009. Albedo estimates for land surface models and support for a new paradigm based on foliage nitrogen concentration. Global Change Biol., doi:10.1111/j.1365-2486.2009.02028.x.
Huemmrich, K.F., Black, T.A., Jarvis, P.G., McCaughey, J.H., Hall, F.G., 1999. High temporal resolution NDVI phenology from micrometeorological radiation sensors. J. Geophys. Res. 104 (D22), 27935–27944.
Huete, A., Didan, K., Miura, T., Rodriguez, E.P., Gao, X., Ferreira, L.G., 2002. Overview of the radiometric and biophysical performance of the MODIS vegetation indices. Remote Sens. Environ. 83, 195–213.
Inoue, Y., Penuelas, J., Miyata, A., Mano, M., 2008. Normalized difference spectral indices for estimating photosynthetic efficiency and capacity at a canopy scale derived from hyperspectral and CO2 flux measurements in rice. Remote Sens. Environ. 112 (1), 156–172.
Kobayashi, H., Dye, D.G., 2005. Atmospheric conditions for monitoring the long-term vegetation dynamics in the Amazon using normalized difference vegetation index. Remote Sens. Environ. 97 (4), 519–525.
le Maire, G., François, C., Soudani, K., Berveiller, D., Pontailler, J.-Y., Bréda, N., Genet, H.e., Davi, H., Dufrêne, E., 2008. Calibration and validation of hyperspectral indices for the estimation of broadleaved forest leaf chlorophyll content, leaf mass per area, leaf area index and leaf canopy biomass. Remote Sens. Environ. 112 (10), 3846–3864.
Leblanc, S.G., Chen, J.M., Fernandes, R., Deering, D.W., Conley, A., 2005. Methodology comparison for canopy structure parameters extraction from digital hemispherical photography in boreal forests. Agric. For. Meteorol. 129 (3–4), 187–207.
Leuning, R., Hughes, D., Daniel, P., Coops, N.C., Newnham, G., 2006. A multi-angle spectrometer for automatic measurement of plant canopy reflectance spectra. Remote Sens. Environ. 103 (3), 236–245.
Ma, S., Baldocchi, D.D., Xu, L., Hehn, T., 2007. Inter-annual variability in carbon dioxide exchange of an oak/grass savanna and open grassland in California. Agric. For. Meteorol. 147 (3–4), 157–171.
Middleton, E.M., 1991. Solar zenith angle effects on vegetation indices in tallgrass prairie. Remote Sens. Environ. 38 (1), 45–62.
Mims, F.M., 1992. Sun photometer with light emitting diodes as spectrally selective detectors. Appl. Opt. 31 (33), 6965–6967.
Mims, F.M., 1999. An international haze-monitoring network for students. Bull. Am. Meteorol. Soc. 80 (7), 1421–1431.
Mims, F.M., 2002. An inexpensive and stable LED Sun photometer for measuring the water vapor column over South Texas from 1990 to 2001. Geophys. Res. Lett. 29 (13), doi:10.1029/2002GL014776.
Morisette, J.T., Richardson, A.D., Knapp, A.K., Fisher, J.I., Graham, E.A., Abatzoglou, J., Wilson, B.E., Breshears, D.D., Henebry, G.M., Hanes, J.M., Liang, L., 2009. Tracking the rhythm of the seasons in the face of global change: phenological research in the 21st century. Front. Ecol. Environ. 7 (5), 253–260.
Nagai, S., Nasahara, K.N., Muraoka, H., Akiyama, T., Tsuchida, S., 2010. Field experiments to test the use of the normalized-difference vegetation index for phenology detection. Agric. For. Meteorol. 150 (2), 152–160.
Nakaji, T., Ide, R., Takagi, K., Kosugi, Y., Ohkubo, S., Nasahara, K.N., Saigusa, N., Oguma, H., 2008. Utility of spectral vegetation indices for estimation of light conversion efficiency in coniferous forests in Japan. Agric. For. Meteorol. 148 (5), 776–787.
Norby, R.J., DeLucia, E.H., Gielen, B., Calfapietra, C., Giardina, C.P., King, J.S., Ledford, J., McCarthy, H.R., Moore, D.J.P., Ceulemans, R., De Angelis, P., Finzi, A.C., Karnosky, D.F., Kubiske, M.E., Lukac, M., Pregitzer, K.S., Scarascia-Mugnozza, G.E., Schlesinger, W.H., Oren, R., 2005. Forest response to elevated CO2 is conserved across a broad range of productivity. Proc. Natl. Acad. Sci. U.S.A. 102 (50), 18052–18056.
Parmesan, C., Yohe, G., 2003. A globally coherent fingerprint of climate change impacts across natural systems. Nature 421 (6918), 37–42.
Peñuelas, J., Rutishauser, T., Filella, I., 2009. Phenology feedbacks on climate change. Science 324 (5929), 887–888.
RayChaudhuri, B., Sen, C., 2009. Light emitting diode as sensor for miniature multispectral radiometer. Appl. Phys. B: Lasers Opt. 95 (1), 141–144.
Rosete-Aguilar, M., Ruiz-Mercado, I., Reygadas, R.F., Velasco-Segura, R., Trjo, Z., Erantzcani, L., 2003. Caracterización espectral, angular y térmica de diodos emisores de luz como detectores ópticos. In: XLVI Congreso Nacional SMF /XVI Reunión Anual AMO, pp. 10V03-1–10V03-10.
Ruiz-Mercado, I., 2005. Diseno construccion de un radiometro solar autonomo que utiliza un arreglo de LEDs como detectores para la medicion de aerosoloes atmosfericos. Universidad Nacional Autonoma de Mexico, Mexico City, Mexico, 94 pp.
Running, S.W., Baldocchi, D.D., Turner, D.P., Gower, S.T., Bakwin, P.S., Hibbard, K.A., 1999. A global terrestrial monitoring network integrating tower fluxes, flask sampling, ecosystem modeling and EOS satellite data. Remote Sens. Environ. 70 (1), 108–127.
Ryu, Y., Baldocchi, D.D., Ma, S., Hehn, T., 2008. Interannual variability of evapotranspiration and energy exchanges over an annual grassland in California. J. Geophys. Res. 113, doi:10.1029/2007JD009263 (D09104).
Ryu, Y., Nilson, T., Kobayashi, H., Sonnentag, O., Law, B.E., Baldocchi, D.D., 2010a. On the correct estimation of effective leaf area index: does it reveal information on clumping effects? Agric. For. Meteorol. 150 (3), 463–472.
Ryu, Y., Sonnentag, O., Nilson, T., Vargas, R., Kobayashi, H., Wenk, R., Baldocchi, D.D., 2010b. How to quantify tree leaf area index in a heterogeneous savanna ecosystem: a multi-instrument and multi-model approach. Agric. For. Meteorol. 150, 63–76.
Sellers, P.J., 1985. Canopy reflectance, photosynthesis and transpiration. Int. J. Remote Sens. 6 (8), 1335–1372.
Sims, D.A., Luo, H., Hastings, S., Oechel, W.C., Rahman, A.F., Gamon, J.A., 2006. Parallel adjustments in vegetation greenness and ecosystem CO2 exchange in response to drought in a Southern California chaparral ecosystem. Remote Sens. Environ. 103 (3), 289–303.
Tilman, D., Reich, P.B., Knops, J., Wedin, D., Mielke, T., Lehman, C., 2001. Diversity and productivity in a long-term grassland experiment. Science 294 (5543), 843–845.
Tucker, C.J., 1979. Red and photographic infrared linear combinations for monitoring vegetation. Remote Sens. Environ. 8 (2), 127–150.
Ustin, S.L., Roberts, D.A., Gamon, J.A., Asner, G.P., Green, R.O., 2004. Using imaging spectroscopy to study ecosystem processes and properties. Bioscience 54 (6), 523–534.
Velasco-Segura, R., 2005. Mediciones de nolinealidad y tiempos de respuesta de diodos emisores de luz. Tesis de Licenciatura de la Carrera de Fisica, Facultad de Ciencias, UNAM.
Velasco-Segura, R., Rosete-Aguilar, M., 2003. Mediciones de no-linealidad de diodos emisores de luz que funcionan como dtectores opticos. In: SOMI XVIII Congreso de Insturmentacion, Ingeniería Óptica, MRA 18169, Mexico, D.F.
White, M.A., Beurs, K.M.d., Didan, K., Inouye, D.W., Richardson, A.D., Jensen, O.P., O'Keefe, J., Zhang, G., Nemani, R.R., Leeuwen, W.J.D.v., Brown, J.F., Wit, A.d., Schaepman, M., Lin, X., Dettinger, M., Bailey, A.S., Kimball, J., Schwartz, M.D., Baldocchi, D.D., Lee, J.T., Lauenroth, W.K., 2009. Intercomparison, interpretation, and assessment of spring phenology in North America estimated from remote sensing for 1982–2006. Global Change Biol., doi:10.1111/j.1365-2486.2009.01910.x.
Xu, L., Baldocchi, D.D., 2004. Seasonal variation in carbon dioxide exchange over a Mediterranean annual grassland in California. Agric. For. Meteorol. 123 (1–2), 79–96.